LAWRENCE
LIVERMORE
NATIONAL
LABORATORY

UCRL-JRNL-221537

Simulations of liquid ribidium expanded to the critical density

M. Ross, L. H. Yang, W.-C. Pilgrim

May 22, 2006

Physical Review B

Updated October 14, 2003

Simulations of liquid rubidium expanded to the critical density

M. Ross and L. H. Yang

Lawrence Livermore National Laboratory, Livermore, CA 94551

W.-C. Pilgrim

Institute of Physical Chemistry and Materials Science Centre,
Philipps-University of Marburg, 35032 Marburg, Germany

Quantum molecular dynamic simulations were used to examine the change in atomic and electronic structure in liquid rubidium along its liquid-vapor coexistence curve. Starting from the liquid at the triple point, with increasing expansion we observe a continuous increase in the electron localization leading to ion clustering near the metal-nonmetal transition at about twice the critical density, in agreement with electrical measurements, and to the presence of dimers near and below the critical density.

I. Introduction

One of the principal reasons for the continued interest in liquid alkali metals is the role they play as model substances to explore the density driven metal to insulator transition. According to Mott[1] this transition should be observed if a metal is expanded continuously by increasing the spacing between the constituent ions. Then, the decreasing density of the conduction electron cloud will increase the localization of the electrons around the ions leading to a discontinuous first order-like transition into an insulating state. Liquid metals were regarded as suitable model systems to prove the validity of the theory because in a liquid the density can be continuously varied along the liquid-vapor equilibrium curve from solid like values close to melting and down to conditions of a dilute gas. Since wide density ranges must be spanned in such experiments, liquid metals are needed in the low density regime close to the liquid vapour critical point that are accessible at temperature and pressure conditions attainable in ordinary laboratory experiments [2,3,4]. The heavier alkali metals,

K, Rb and Cs, with critical temperatures 2178 K, 2017 K and 1924 respectively, are well suited for this undertaking.

However, density dependent measurements of the dc-electrical conductivity[5] and the magnetic susceptibility [6] of fluid cesium show that the transition is continuous, rather than first order sharp-like, as predicted by Mott. For example, liquids do not generally decrease their density by simply increasing the inter-particle distances, but rather by decreasing the coordination number and forming local molecular aggregates. Information on how the liquid alkali metal structure changes in the expanded phase may be gleaned from magnetic and electrical measurements. They indicate that the electrical conductivity of expanded alkalis begin to transform from that of a nearly free electron (NFE) liquid state at densities below three times the critical value [5]. This is believed due to the continuing loss of conduction electrons due to aggregate formation. With a further reduction in density towards the critical value the paramagnetic magnetic susceptibility continues to increase indicating a rising number of electrons localizing at their parent ions. In fact dimer-monomer equilibria is a well known feature of the dilute alkali metal gas phase, where all electrons are localized and the dimers are clearly insulating[4]. However, a detailed understanding of how the local atomic structure changes from liquid metal to dimer gas remains uncertain.

Some indication as to the specific nature of molecular units that may form under expanded conditions was obtained in an earlier paper [7,8] where measurements of the vibron energy in such units made by inelastic neutron scattering (INS) were reported. These measurements were made at several points, shown in figure 1, along the experimental liquid-vapor coexistence data curve [3]. They lie in the density range of 0.61 g/cm^3 to 0.5 g/cm^3, near twice critical density. Rubidium has a critical temperature and density of $T_c = 2017\ K$, and $\rho_c = 0.29\ g/cm^3$[3]. Calculations reported earlier [7,8] of the total energy for expanded lattices of Rb atoms and Rb_2 molecules, and shown in figure 2, predicted that for densities below $0.8 g/cm^3$ the molecular lattice would have the lower energy. The values of the calculated Rb_2 vibron energies are in excellent agreement with the INS measurements. Although the predictions of the lattice

models provide some theoretical support for the presence of dimers in the expanded state, the neglect of liquid structure and thermal properties represents a serious omission.

At a more fundamental level, density-functional-theory quantum molecular dynamics (DFT-MD) provides a method that allows for a *first-principles* simulation of electronic energy coupled with the nuclear motion. Shimojo et al.[9] have reported the results of simulations for liquid Rb at the triple point (350 K, 1.459 g/cm^3) and at 1400 K (0.97 g/cm^3). At the triple point Rb exhibits the behavior of a typical monatomic alkali metal liquid, with the charge density spread over space except in the neighborhood of well separated ions. At an expanded density of 0.97g/cm^3 they found a tendency for the electronic charge to begin to localize. Alemany et al.[10] extended the range covered by Rb simulations to 0.61 g/cm^3 where they reported observing clusters in their contour snapshots that they interpreted as trimers.

In order to more fully understand the nature of the very highly expanded metal, we have undertaken simulations that extend the degree of expansion to the critical density, ρ_c=0.29 g/cm^3, and beyond to 0.145 g/cm^3, where it appears only isolated dimers exist. In section II, we report these results and discuss their significance in terms of prior experimental findings. Some of our preliminary simulation results have been reported [11]. Section III is the Discussion.

II. Quantum molecular dynamic computer simulations and neutron scattering measurements

DFT-MD calculations were made for liquid Rb employing essentially the same method as Shimojo et al.[9]. We used a plane-wave pseudo-potential code with 64 atoms in the unit cell and a fixed plane-wave cutoff at 80 Ryd which is sufficient for a Rb pseudopotential generated with 7 valence electrons, with time steps of 0.75 fs. A few calculations including 128 atoms were also made to check size effects. At each time step the energy, forces and electron band structure were calculated. After achieving thermal equilibration, the system properties, including the total electron density of states (TEDOS) were obtained by averaging over the final 3,000 time steps using ionic temperatures as the

smearing function. Simulations were made at several densities along the liquid-vapor coexistence data. The most revealing information is the variation of the structural distribution of the ion and electron densities observed in the electron-ion contour plot snapshots in figures 3 a-d and of the TDEOS, in figure 4, near the metal-nonmetal transition.

At the triple point ($1.459 g/cm^3$) rubidium is considered to be a simple monatomic liquid(figure 3a). However, while the ions appear to be randomly dispersed the electron density is not smoothly distributed, but is interconnected throughout the liquid and there appears to be some clustering between neighboring ions even at the normal liquid density. A similar behavior of the electron contours is observed in the calculations by Shimojo et al[9]. This is in accord with structural investigations employing static x-ray and neutron scattering techniques[12] which also indicate the liquid alkalis are simple monatomic under these conditions. The dynamic scattering law $S(Q,\omega)$ exhibits distinct excitation peaks resulting from the creation and annihilation of small wavelength sound modes[13]. Whether these collective dynamics may be related to the calculated contours is beyond the scope of the present paper. While the precise nature of the collective excitations is not yet fully understood, their influence gradually vanishes with increasing temperature and expansion.

The contour plot in figure 3b shows that at $0.97 g/cm^3$, slightly more than three times the critical density, there is a rise in electron localization coinciding with an observed drop in the electrical conductivity[5], and a rise in magnetic susceptibility[6]. Also, an unusual pile up of charge on a sub-picosecond timescale is observed between approaching ions, which might be interpreted as the onset of a tendency to form molecular aggregates. Shimojo et al.[9] made a similar observation. These short time correlations do not show any trace in the experimental $S(Q,\omega)$ measured under similar conditions. However, this does not conflict with the simulation results, since the neutron experiment does not cover the required time scale to observe these correlations. The measured $S(Q,\omega)$-spectra are simple shaped and considerably broadened due to the high temperatures. They are still characteristic of a typical monatomic fluid with a rapid decay of the microscopic density-density correlation.

If the density is further decreased to near twice the critical value then significant changes are observed in the shape of the inelastic neutron spectra[7,8]. At 0.61 g/cm^3(1873 K), 0.58 g/cm^3(1923 K) and 0.5 g/cm^3 (1973 K) distinct peaks are observed in the current correlation spectra $J_l(Q,\omega) = \omega^2/Q^2 \cdot S(Q,\omega)$. The corresponding frequencies and Q-behavior of the measured intensities are conformed with a simple model [14] identifying the peaks as resulting from the excitations of a local vibron indicating. The appearance of a vibron in the scattering measurements may interpreted as resulting from the presence of a local structure. A slight shift to a higher vibron frequency, due presumably to stronger bonding, is observed if the density is decreased form 0.61 g/cm^3 to 0.5 g/cm^3. The earlier calculations of vibron energies in Rb_2-lattices reproduced the observed frequency shift surprisingly well[7,8]. The snapshot in figure 3c at 0.58 g/cm^3, and simulations by Alemany et al.[10] near 0.61 g/cm^3, both predict clustering near this density.

Some additional evidence supporting a transition in the chemical bonding comes from an examination of the TEDOS, shown in figure 4. The TEDOS curve at 0.58 g/cm^3 exhibits a linear increase with increasing energy, while in the TEDOS at 0.47 g/cm^3 a distinct peak shows up near the Fermi surface, indicating the formation of a bound state. Although these smoothed curves represent the configuration averaged values of the simulations, the appearance of a clearly distinct peak near the Fermi energy is apparent in the raw data at 0.47 g/cm^3, but not at 0.58 g/cm^3. A failure of the simulations to predict a TEDOS peak in the simulations at 0.58 g/cm^3 conflicts with the appearance of a vibron in the neutron scattering experiments at that density [7,8]. This brings into question the reliability of the DFT-MD method. The method relies on the Kohn-Sham approximation to the exchange-correlation energy functional. The KS method has been criticized with regard to its usefulness in thermo-chemical applications in predicting the relative stability of chemical systems [15]. Particularly of weakly bound systems. We interpret the lack of a vibron in the simulations at 0.58 g/cm^3 to mean that at this density, and higher, Rb clusters are not bound states, but scattering states. Nevertheless, using the KS approximation does provide a convenient semi-quantitative method for treating complex chemical equilibria.

Upon further expansion of the Rb fluid to near the critical density, at 0.29g/cm^3, stable dimers appear (figure 3d). An examination of the pair distribution at half critical density (0.145 g/cm^3) shows the passage to a dilute gas at the lower density. The calculated nearest neighbor bond distance is 4.5 Å, which indicates that the inter-particle distance changes very little with decreasing density from its liquid metal value of 4.8 Å. The gas phase value of the Rb_2 bond distance is 4.2 Å. The trend of a small change in the liquid to gas value of the bond distance is consistent with a physical model in which the expansion occurs with the formation of molecular aggregates. This trend has also been observed by others [2].

III. Discussion

Overall, experimental measurements and computer simulations agree that a metal-nonmetal transition occurs near twice the critical density in the range of 0.6 g/cm^3 to 0.5 g/cm^3, and the simulations predict that dimers are the predominate species near the critical density. Some additional insight regarding the transition may be gained from an inspection of the rubidium isochoric measurements of Jungst et al.[3] as tabulated in Hensel and Warren [2]. Jungst et al. succeeded in measuring the isochores of the expanded metal over a wide range of densities and pressures. Their data can be expressed in terms of the general thermodynamic relation with the help of the equation,

$$P = \gamma_V T - P_i = (\partial P/\partial T)_V T - (\partial U/\partial V)_T,$$

where $\gamma_V = (\partial P/\partial T)_V$ is the isochoric thermal pressure coefficient. $P_i = (\partial U/\partial V)_T$, which is the internal pressure, and is a measure of the variation of the internal energy (U) or binding energy with expansion. We have plotted $(\partial U/\partial V)_T$ versus density in figure 5. The plot shows two distinct linear regimes connected by a smoothly varying passage. In the higher density range, above 0.5 g/cm^3, Rb is metallic and below a density of 0.3 g/cm^3 it is mainly a dimer-like gas. We identify the intermediate regime with the formation of clusters predicted from computer simulations.

Redmer and Warren[16] carried out model calculations in which they treated expanded liquid *Rb* and *Cs* as partially ionized plasmas, a mixture of

ionized and neutral atoms, dimers, charged dimers and free electrons. They found an enhancement of the electronic magnetic susceptibility at about 2-3 times the critical density, which can be explained by assuming the formation of Cs_2^+ and Rb_2^+. The concentration of charged dimers peaked near twice critical density. Rb_2 and Rb were the principal components of the vapor near and below the critical density, similarly for cesium. While the dense plasma approach is not well suited to treat molecular clustering or liquid metals, by specifically including thermal electron excitation and ionization, it may be the more appropriate model for use at the lowest densities. In effect, expanded alkali metal research spans the range of physics from condensed matter to dense plasmas.

Viewed in a density reversed frame of reference, compression of Rb starting from the dilute diatomic gas to the metallic liquid phase, the changes in structure bears a strong resemblance to recent studies by Eremets et al. [17] in which compressing solid molecular N_2 leads first to an intermediate polymeric phase, before becoming metallic. This would be roughly the same sequence of states tracked by compressing Rb_2 from the gas phase. It is has also been suggested, on the basis of theoretical calculations, that shock compressed D_2 starting in the liquid at 20 K follows a similar sequence of states by passing from a molecular phase to a fluid with chain-like aggregates prior to becoming a dense plasma at megabar pressures [18].

Acknowledgments – We wish to thank Prof. Friedrich Hensel for many valuable discussions. The work of MR and LHY was partially supported under the auspices of the U.S. Department of Energy by the University of California Lawrence Livermore National Laboratory under contract No. W-7405-ENG-48.

References

1. N.F. Mott Proc. Phys. Soc. London, **62**, 419 (1949); N.F. Mott, "Metal-Insulator Transitions", London, Taylor and Francis (1974).

2. F. Hensel and W.W. Warren, Jr., *Fluid Metals* (Princeton University Press, Princeton, NJ, USA, 1999.

3. S. Jüngst, B. Knuth and F. Hensel, Phys. Rev. Lett. **55**, 2160 (1985).

4. C.T. Ewing, J.P. Stone, J.R. Spann and R.R. Miller, J. Phys. Chem. 71, 473 (1967).

5. F. Noll, W-C Pilgrim and R. Winter, Z. Phys. Chem. N.F. **156**, 303 (1988).

6. W. Freyland, Phys. Rev. B **20**, 5104 (1979); J. Phys. (Paris) Colloq. **41** C-8:74 (1980).

7. W-C. Pilgrim, M. Ross, L.H. Yang and F. Hensel, Phys. Rev. Lett. **78**, 3685 (1997)

8. W.-C. Pilgrim, M. Ross, L. H. Yang, Physica B 241-243, 935 (1998).

9. F. Shimojo, Y. Zempo, K. Hoshino and M. Watabe. Phys. Rev. B **52**, 9320 (1995); J. Non-Cryst. Solids, **205-207**, 893 (1996).

10. M.M.G. Alemany, J.L. Martins and B.J. Cabral, J. Non-Cryst. Solids, **347**, 100 (2004).

11. 15. W.-C. Pilgrim and C. Morkel (submitted to J. Phys.:Condensed Matter).

12. W.v. der Lugt, B. P. Alblas, *Handbook of Thermodynamic and Transport Properties of the Alkali Metals* ed R Ohse (Blackwell Scientific Publications) p 299, 1985)

R. Winter, T. Bodensteiner, W. Gläser and F. Hensel, Ber. Bunsenges. Phys. Chem. **95** 1133 (1987), G. Franz, W. Freyland, W. Gläser, F. Hensel and E. Schneider, *J. Phys. Colloq.* **41** 194 (1980)

13. J. R. D. Copley, J. M. Rowe, *Phys. Rev. Lett.* **32** 49 (1974); T. Bodensteiner, Chr. Morkel, W. Gläser, *Phys. Rev.* A **45** 5709 (1992); H. Sinn et al., Phys. Rev. Lett. **78** 1715 (1997); W.-C. Pilgrim, S. Hosokawa, H. Saggau, H. Sinn, E. Burkel, *J.* Noncryst. Solids **250-252** 96 (1999); T. Scopigno, U. Balucani, G. Rocco, F. Sette Phys. Rev. Lett. **85** 4076 (2000).

14. S.W. Lovesey, in "Theory of Neutron Scattering from Condensed Matter", Oxford Science Publications (1986).

15. A. D. Boese and J. M. L. Martin, J. Chem. Phys. **121**, 3405 (2004), and references therein.

16. R. Redmer and W.W. Warren, Jr., Phys. Rev. B **48**, 14892 (1993).
17. M. I. Eremets, A.G. Gavriliuk, I.A. Trojan, D.A. Dzivenko, R. Boehler, Nature Materials,3, 558 (2004); M. I. Eremets, A.G. Gavriliuk, N.R. Serebryanaya, I.A. Trojan, D.A. Dzivenko, R. Boehler, H-k Mao and R.J. Hemley, J. Chem. Phys. **121**, 11296 (2004).
18. M. Ross and L.H. Yang, Phys. Rev. B **64**, 134210 (2001).

Figure captions

Fig. 1. Rubidium liquid-vapor coexistence curve. Experimental measurements are shown by the solid curve[3]. Densities at which DFT-MD simulations were made are indicated by filled circles,●. Points at which oscillator frequencies were measured by inelastic neutron scattering are represented unfilled squares, □, [7,8].

Fig. 2. Total energy for expanded lattices of *Rb* atoms and Rb_2 molecules [7,8].

Fig. 3. Contour snapshots of ion positions (filled circles) and electron density contours. Ions are indicated by black circles and the electron densities decrease as ROYGBIV; a) $1.459 g/cm^3$, b) $0.97 g/cm^3$, c) $0.58 g/cm^3$ and d) $0.29 g/cm^3$. Spatial coordinates are in Ångstroms.

Fig. 4. Total Electron Density of States (TEDOS) plotted versus energy, at densities of 0.58 g/cm^3 (dashed curve) and 0.467 g/cm^3(filled circles). Energies are set relative to the Fermi energy, = 0.0 eV (vertical dashed line).

Fig. 5. Internal pressure of liquid and vapor rubidium plotted versus density [2].

Fig. 1

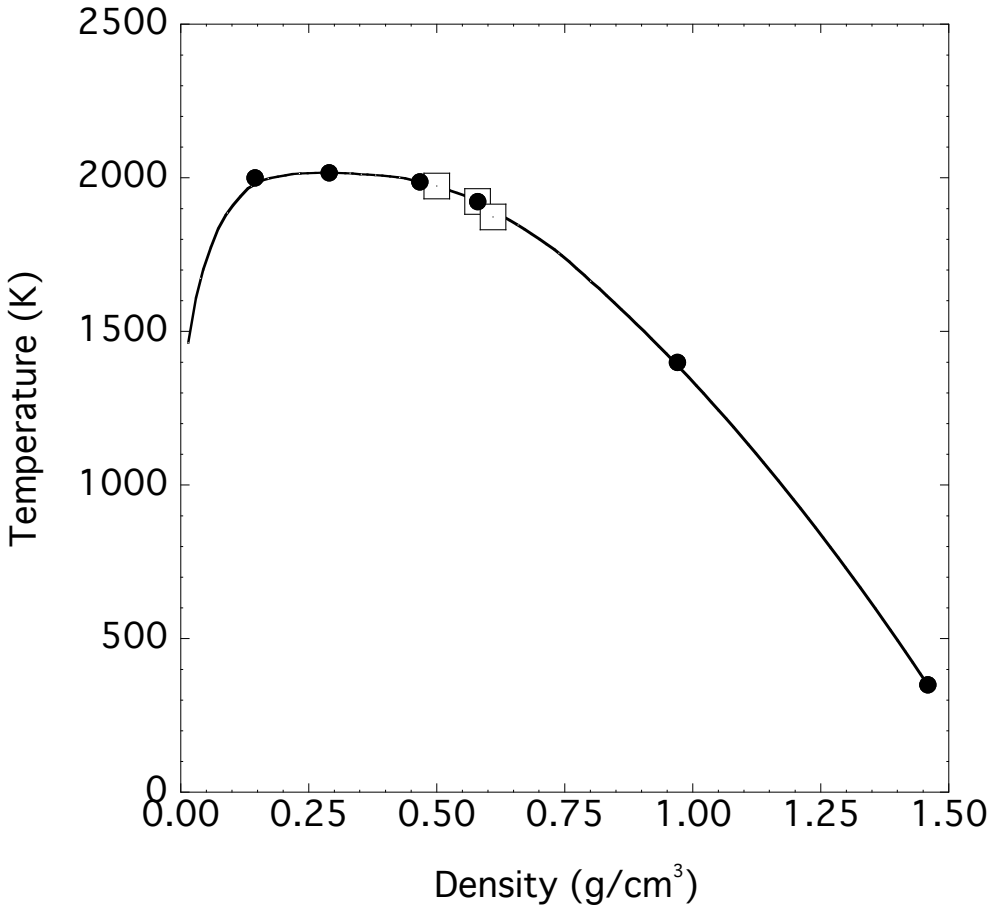
2500
2000
1500
1000
500
0
Temperature (K)
0.00
0.25
0.50
0.75
1.00
1.25
1.50
Density (g/cm3)

Fig. 2

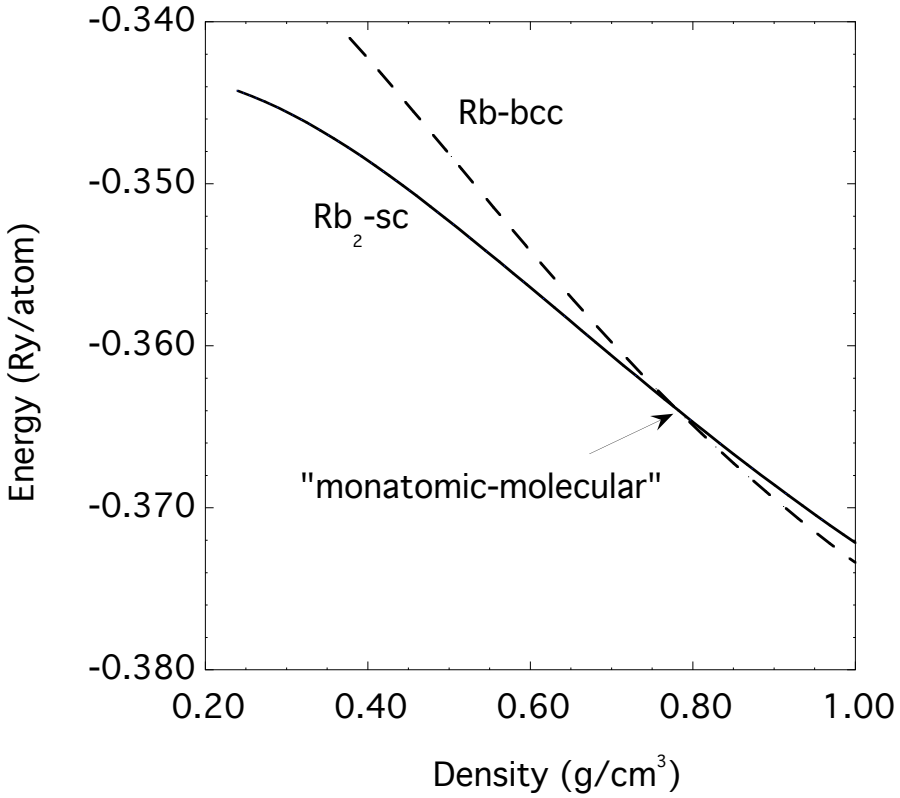
-0.340
-0.350
-0.360
-0.370
-0.380
0.20
0.40
0.60
0.80
1.00
Energy (Ry/atom)
Density (g/cm3)
Rb-bcc
Rb2-sc
"monatomic-molecular"

Fig. 3a

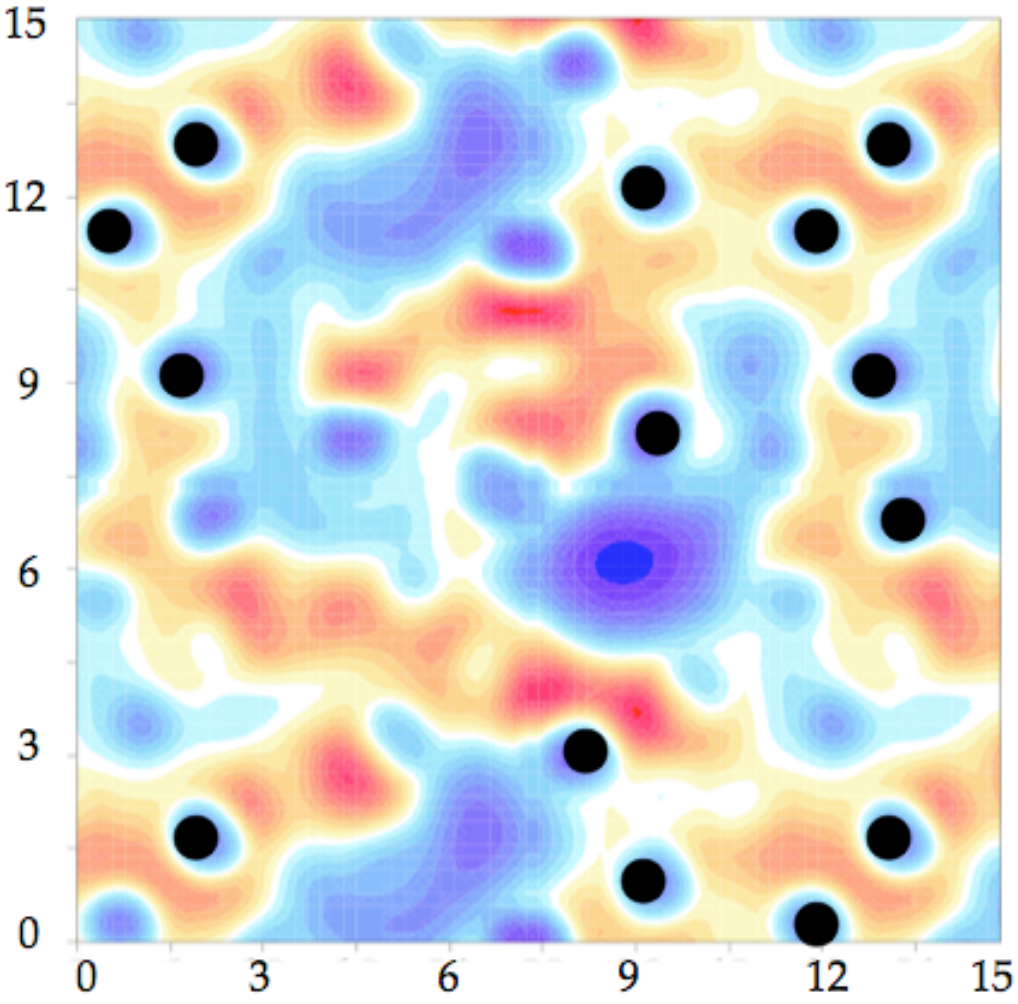

Fig. 3b

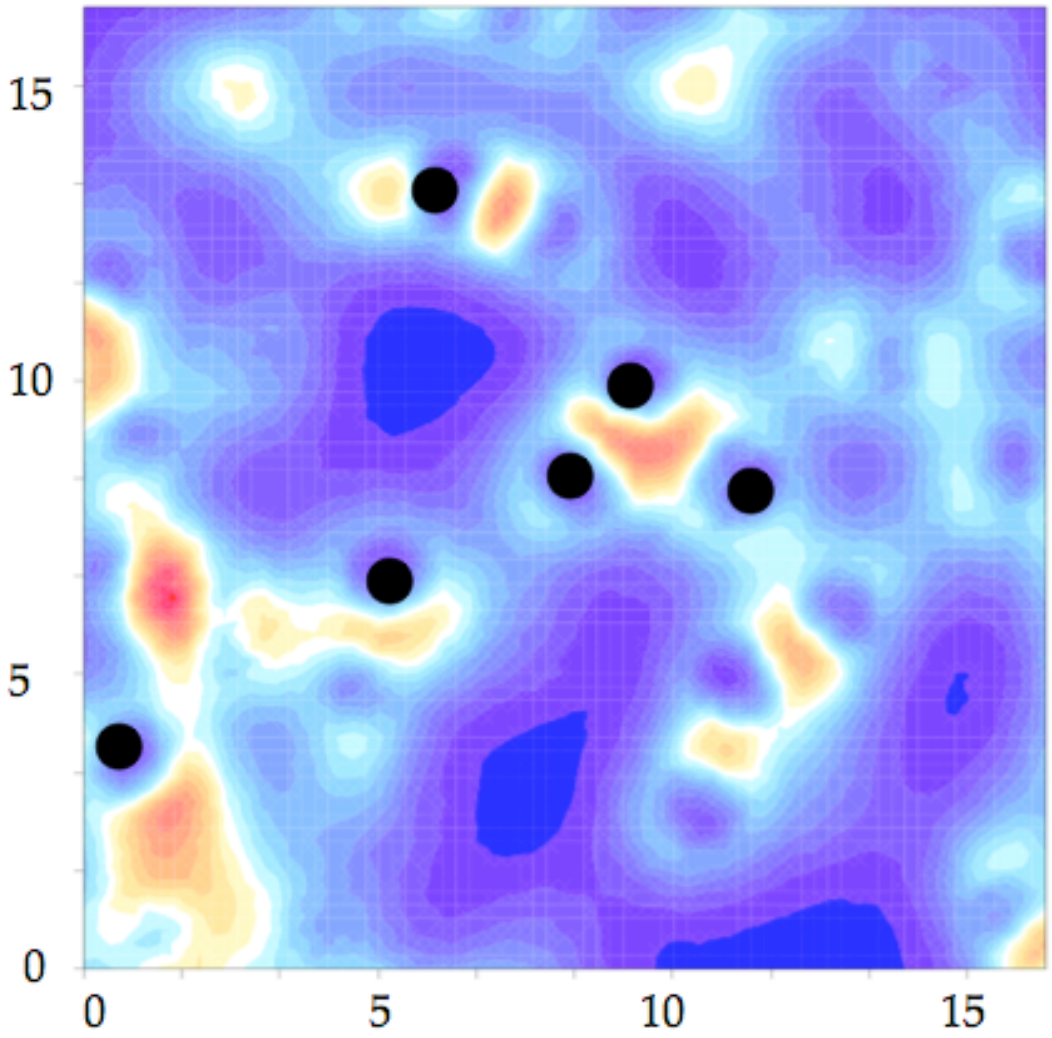

Fig. 3c

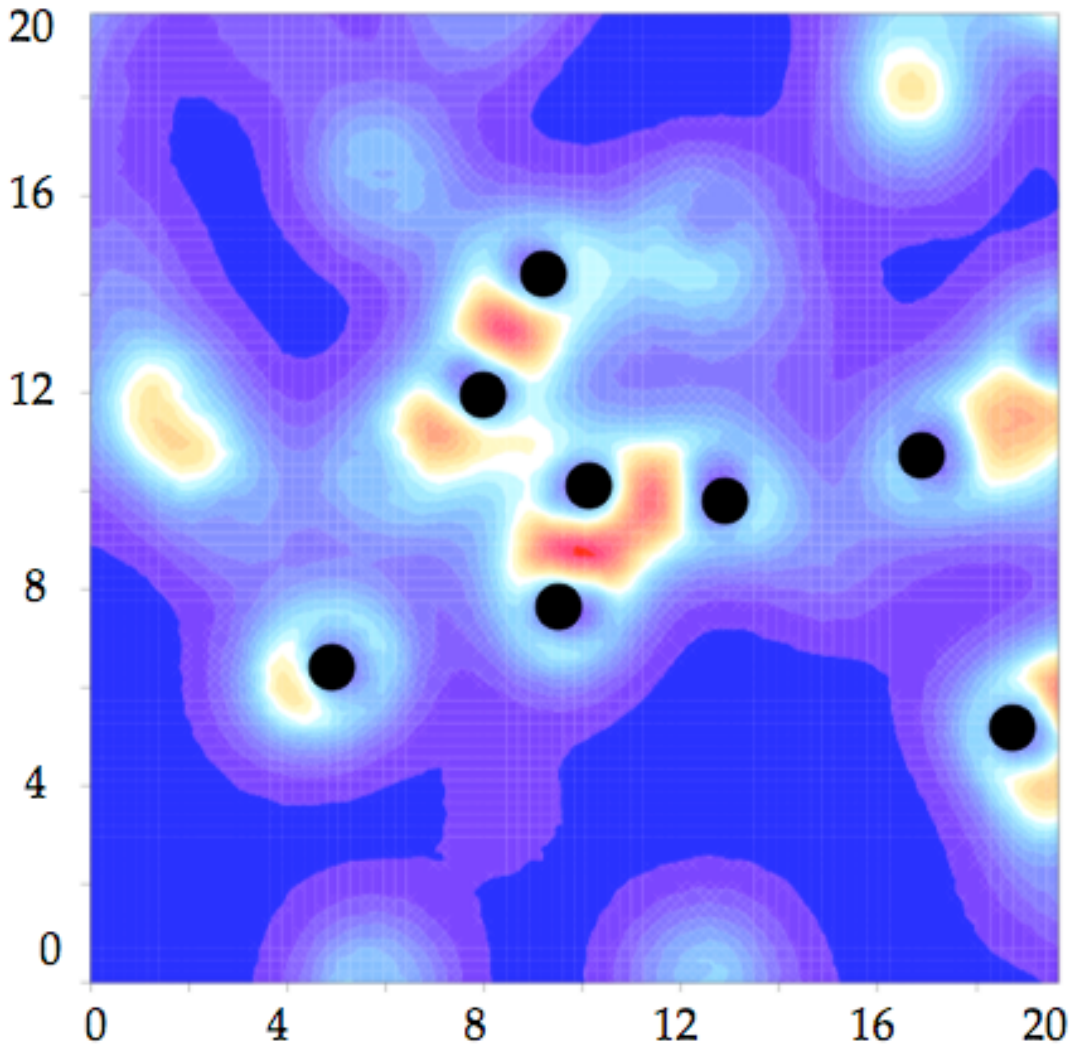

Fig.3d

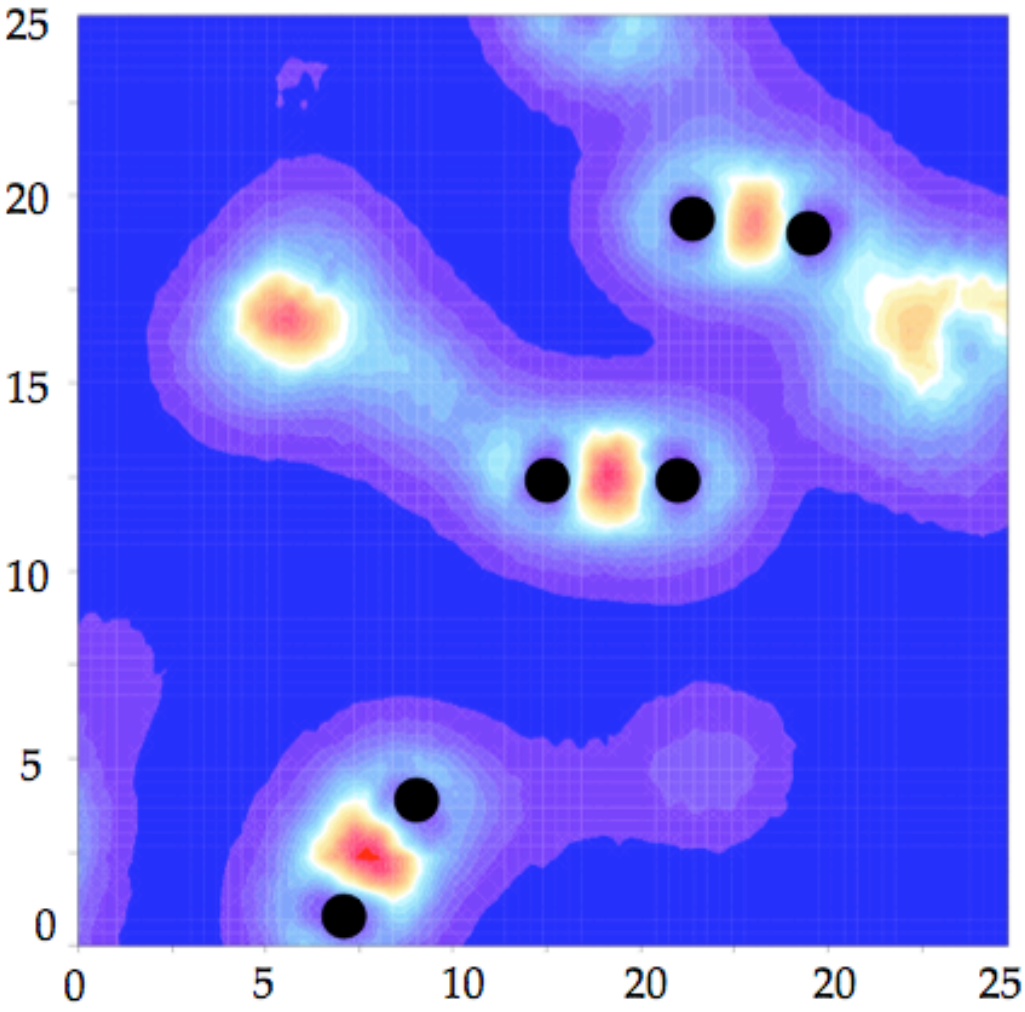

Fig. 4

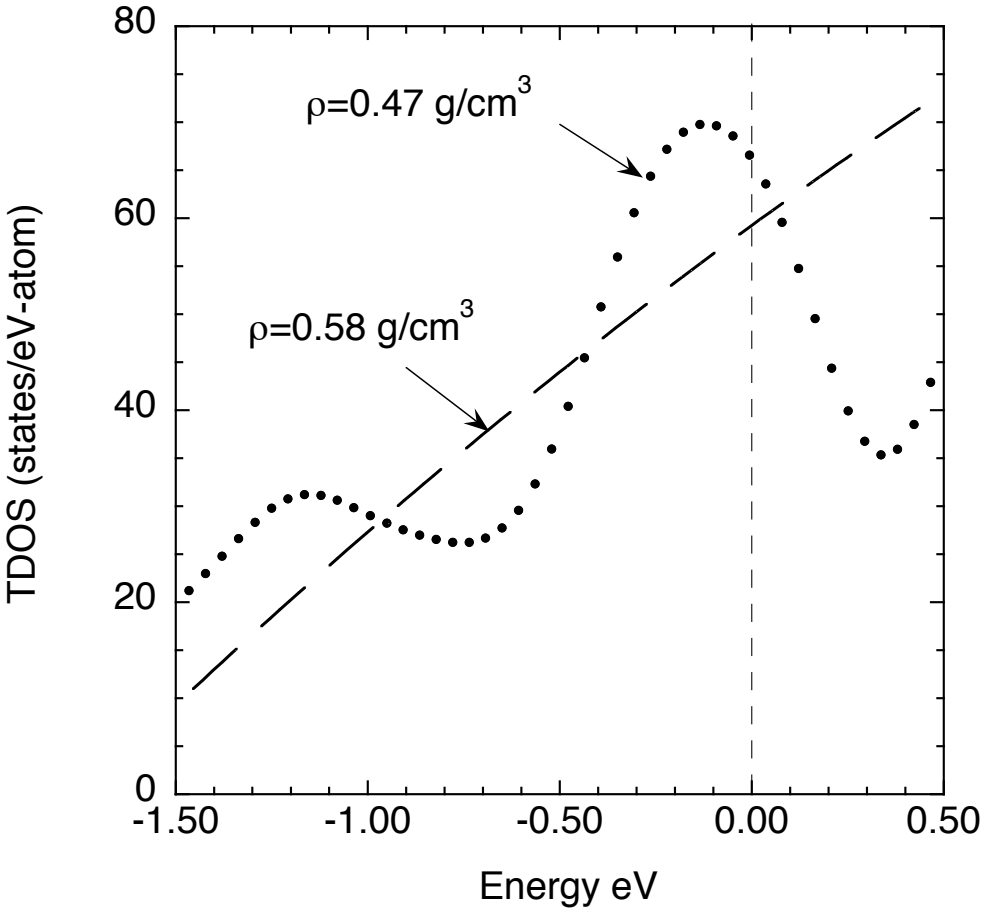
80
60
40
20
0
TDOS (states/eV-atom)
ρ=0.47 g/cm3
ρ=0.58 g/cm3
-1.50
-1.00
-0.50
0.00
0.50
Energy eV

Fig 5.

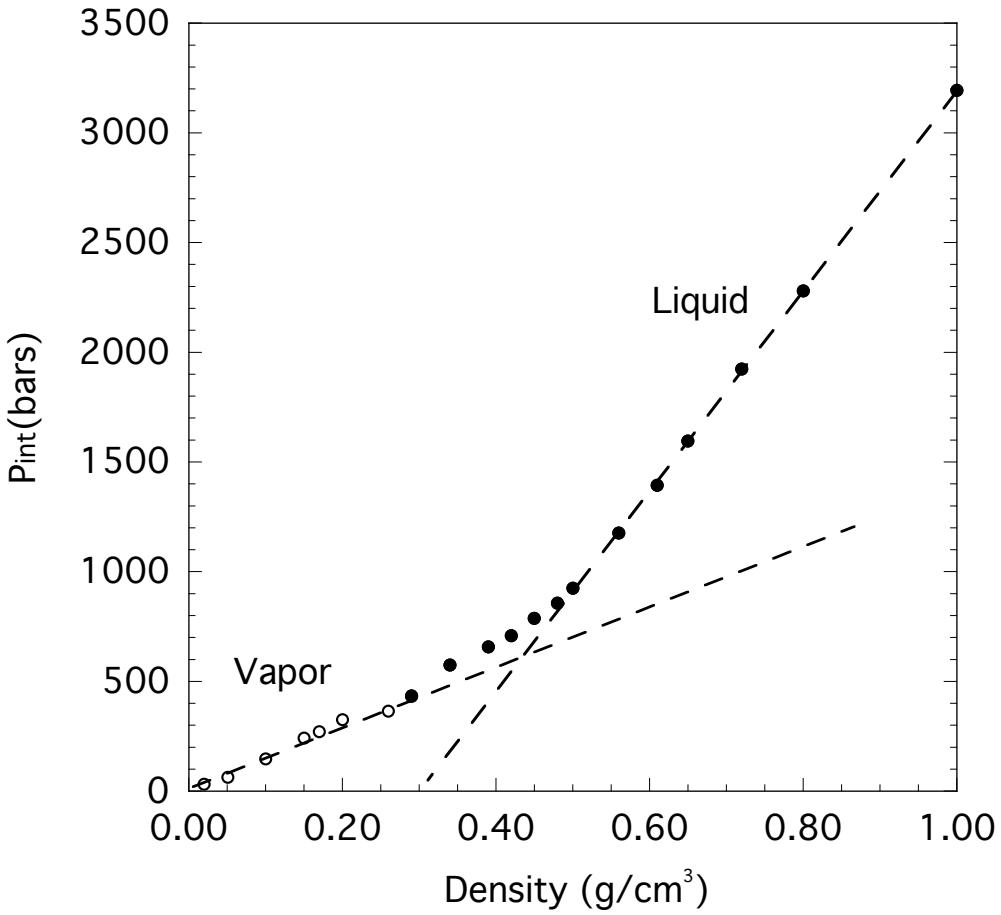
3500
3000
2500
2000
1500
1000
500
0
P_{int}(bars)
Liquid
Vapor
0.00
0.20
0.40
0.60
0.80
1.00
Density (g/cm^3)